Journal of Crystal Growth 378 (2013) 571–575

Contents lists available at SciVerse ScienceDirect

Journal of Crystal Growth

journal homepage: www.elsevier.com/locate/jcrysgro

Long-wavelength electroluminescence of InGaAs-capped type-II GaSb/GaAs quantum-rings at room temperature

Wei-Hsun Lin [a], Kai-Wei Wang [b], Shih-Yen Lin [c,d,e,*], Meng-Chyi Wu [a]

[a] Institute of Electronics Engineering, National Tsing Hua University, Hsinchu 300, Taiwan
[b] College of Photonics, National Chiao-Tung University, Tainan 711, Taiwan
[c] Research Center for Applied Sciences, Academia Sinica, Taipei 11529, Taiwan
[d] Department of Photonics, National Chiao-Tung University, Hsinchu 300, Taiwan
[e] Institute of Optoelectronic Sciences, National Taiwan Ocean University, Keelung 20224, Taiwan

ARTICLE INFO

Available online 3 January 2013

Keywords:
A1. Nanostructures
B1. Antimonides
A3. Molecular beam epitaxy
B2. Semiconducting III–V materials

ABSTRACT

The room-temperature photoluminescence (PL) and electroluminescence (EL) exceeding 1.3 μm are observed for InGaAs-capped GaSb quantum-ring (QR) structures. With increasing In composition, the emission wavelength would shift from 1.18 to 1.31 μm. The InGaAs-capped GaSb QRs also exhibit a higher injection current and stronger EL intensity at the same applied voltage. With the observation of low-temperature PL spectra, the transition mechanisms of the standard and InGaAs-capped QRs are further investigated.

© 2012 Elsevier B.V. All rights reserved.

1. Introduction

Antimonide-based nanostructure such as GaSb/GaAs quantum dots (QDs) has attracted much interest due to their staggered (type-II) band alignment and large valence-band offset [1–5]. By using this nanostructure, some groups have proposed that with the incorporation of type-II GaSb QDs into a type-I InGaAs quantum well (QW), the emission wavelength can be extended to 1.6–1.7 μm in theory [6,7]. However, only few papers have been published in recent years regarding the long-wavelength emission of type-II nano-structures. The main issue responsible for this phenomenon is the severe As/Sb exchange and Sb segregation between GaSb/GaAs interfaces, which would generate dislocations along the hetero-structure and degrade the crystalline quality of the nano-structures [8–10]. In our previous study, we discovered that by using the procedure of long post-growth Sb soaking, intense room-temperature photoluminescence (PL) and electroluminescence (EL) of GaSb QDs were observed [11]. It has also been demonstrated that by controlling the flux ratio of Sb to background As during the post-growth Sb soaking procedure, either dots or rings can be obtained [12]. Moreover, GaSb quantum rings (QRs) exhibit the more intense PL than QDs do. In this case, if the emission wavelength of GaSb QRs can be pushed to communication wavelengths, the type-II GaSb nano-structures can be very useful in the near infrared range.

In this article, we investigate the influence of In composition of the InGaAs capping layers on the performance of type-II GaSb/GaAs QR structures. With increasing In composition of the InGaAs capping layer, a red shift of PL peak is observed at room temperature. Also observed is the larger blue shift of the InGaAs-capped QR structure in the same pumping power span, which suggests a higher number of electron–hole pairs accumulated at the interfaces. The transition mechanisms of standard and InGaAs-capped GaSb/GaAs QRs are investigated with the observation of PL spectra at low temperatures. By fabricating the sample into a diode, a longer EL emission wavelength and an intense EL intensity are observed for the InGaAs-capped QR structures.

2. Experiment

The samples investigated in this study were grown on (100)-orientated semi-insulated GaAs substrates by using a solid source molecular beam epitaxy system. In this system, the As and Sb sources both were adopted to a valve cracker cell to control the atom flux. Three 3-period GaSb/GaAs QR samples with different

Table 1
The wafer structures of samples A, B and C.

Sample	A	B	C
3.0 ML GaSb QRs			
40 nm GaAs			
10 nm $In_xGa_{1-x}As$ Capping Layer	X=0	X=0.1	X=0.15
3.0 ML GaSb QRs			
200 nm undoped GaAs			
350 nm GaAs S-I substrate (001)			

x3

* Corresponding author at: Research Center for Applied Sciences, Academia Sinica, 128 Section 2, Academia Road, Nankang, Taipei 11529, Taiwan. Tel.: +886 3 5744364; fax: +886 3 5745233.
E-mail address: shihyen@gate.sinica.edu.tw (S.-Y. Lin).

0022-0248/$ - see front matter © 2012 Elsevier B.V. All rights reserved.
http://dx.doi.org/10.1016/j.jcrysgro.2012.12.066

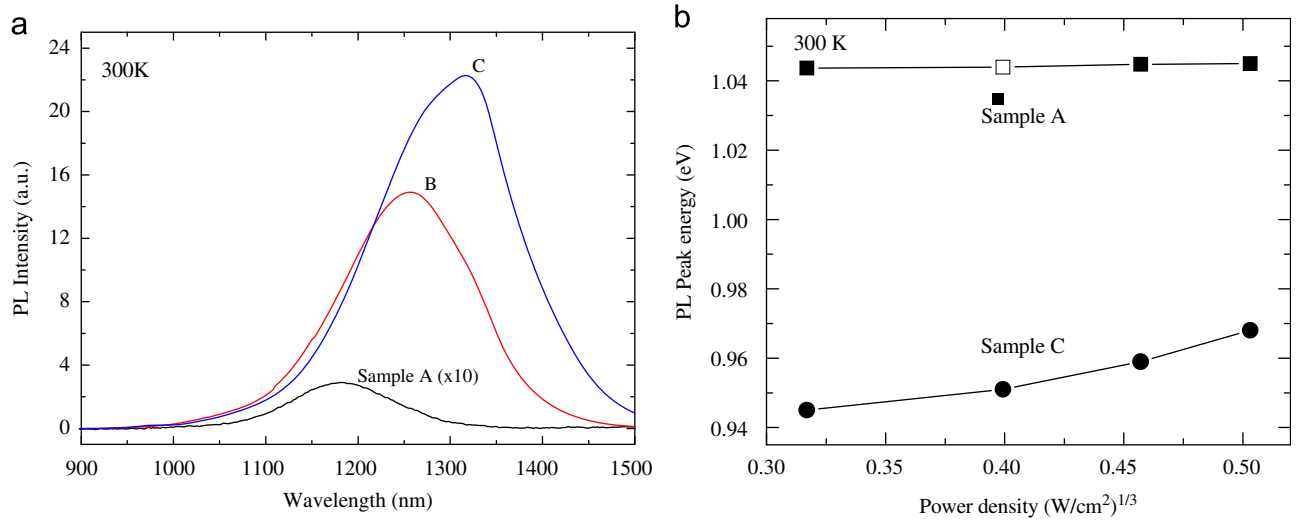

Fig. 1. (a) The PL spectra of sample A, B and C at room temperature at a laser pumping power of 0.5 W/cm^2 and (b) the PL peak energy of samples A and C as a function of cubic root of pumping intensity.

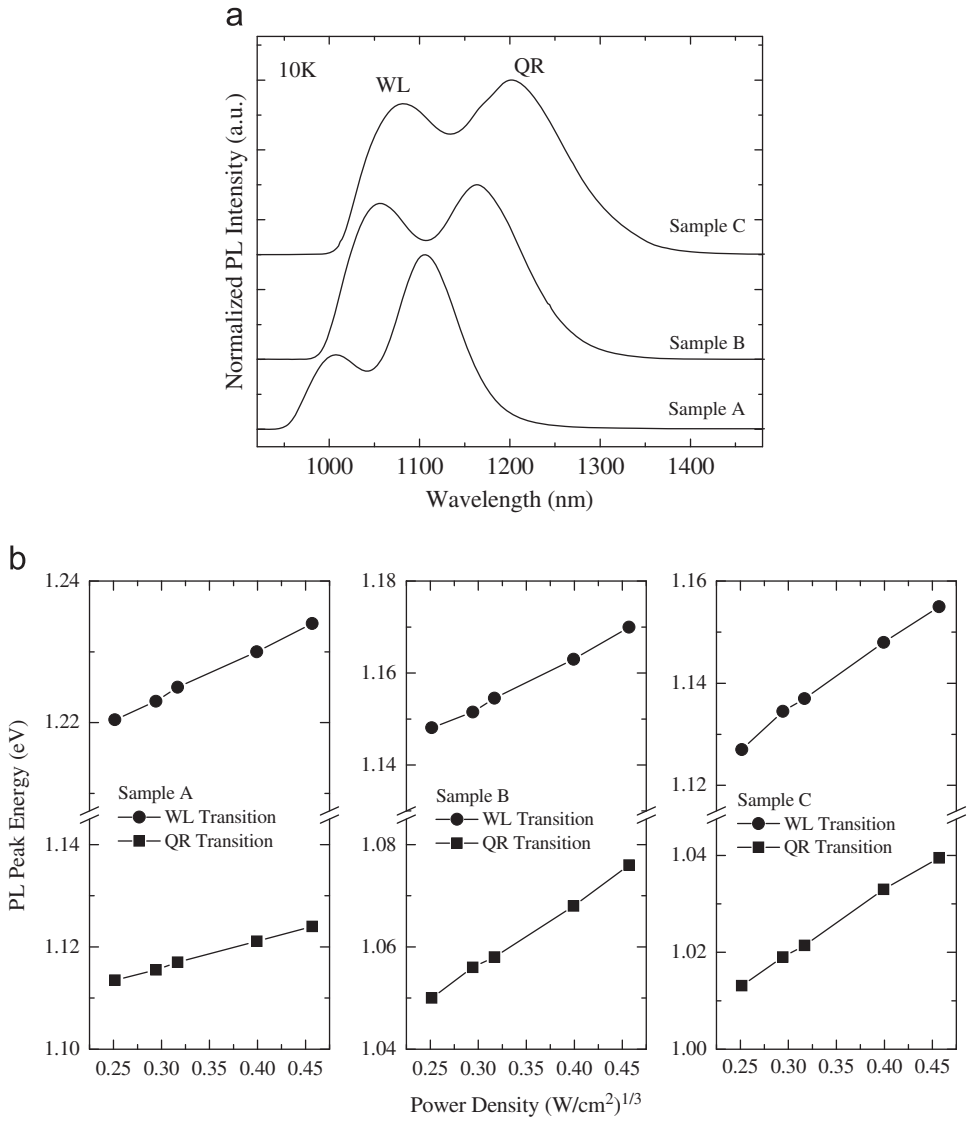

Fig. 2. The normalized PL spectra of samples A, B and C at 10 K at a laser pumping power of 0.5 W/cm^2.

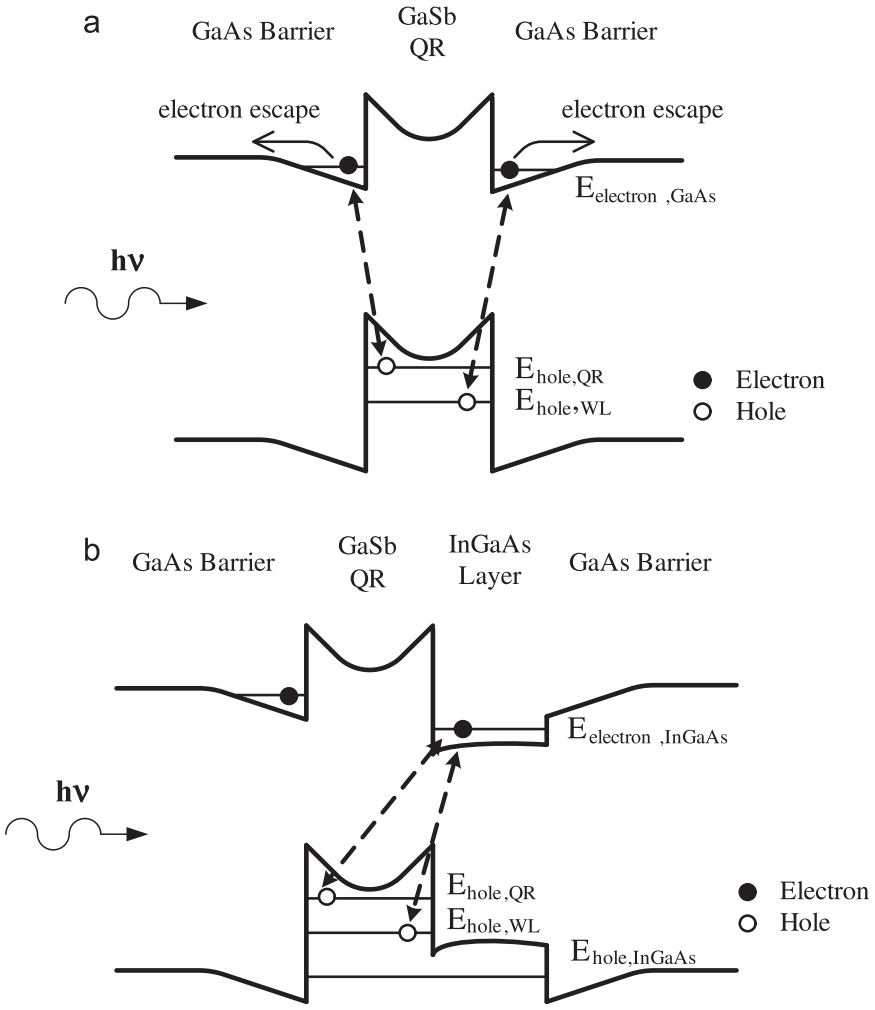

Fig. 3. The schematic band diagram of: (a) standard and (b) InGaAs-capped QR structures.

capping layers of GaAs, $In_{0.1}Ga_{0.9}As$ and $In_{0.15}Ga_{0.85}As$ were prepared, which are referred as samples A, B and C, respectively. The wafer structures are shown in Table 1. After growing a 200-nm thick buffer layer at 580 °C, the substrate temperature was ramped down to 470 °C for subsequent QD growth. In these three samples, GaSb QD was grown by depositing 3.0 monolayers (ML) of GaSb at a deposition rate of 0.75 ML/s. After QD growth, 120-s post soaking of Sb was performed with a well-controlled flux ratio of Sb to background As such that full ring morphology can be obtained for all the three samples. The detail growth procedures are discussed elsewhere [12]. Subsequently, 10 nm-thick capping layer was grown. Finally, the substrate temperature was ramped up to 580 to grow the 40 nm-thick GaAs layer. Additional GaSb QR structures were grown on top of the three samples for the atomic-force microscopy (AFM) measurements. The PL measurements were performed by using the Jobin Yvon's NanoLog3 system coupled with HeNe laser as the pumping source. The EL measurements were performed by using the Jobin Yvon's NanoLog3 system coupled with Keithley 2602.

3. Results and discussion

The room-temperature PL spectra of samples A, B and C at a laser pumping power density of 0.5 W/cm^2 are shown in Fig. 1(a). Distinctive red shift of emission wavelength from 1.18 to 1.31 μm with increasing In composition is observed. The phenomenon is attributed to the lowering conduction-band edge of the InGaAs capping layer with increasing In composition such that a reduced energy difference between electron and hole states is observed. On the other hand, no PL signal resulted from the type-I InGaAs QW is observed in this figure, which indicates that the optical recombination probability of electron–hole pairs in the InGaAs QW is smaller. A possible mechanism responsible for this phenomenon is the easy relaxation of holes from InGaAs QW to GaSb QRs. In this case, the dominated PL peak observed in Fig. 1(a) is resulted from the optical recombination of localized holes in QRs and the electrons in InGaAs QW. To verify if the PL peak is resulted from type-II transitions, the PL peak energies of samples A and C as a function of the cubic root of laser pumping power density are shown in Fig. 1(b). In this figure, while similar PL peak energies of ~1.04 eV are observed for sample A, a larger blue shift of 20 meV in the same pumping power span is observed for sample C. This result is attributed to the increase of electron–hole pairs accumulated at the (InGa)As/GaSb interfaces, which is resulted from the better confinement of the InGaAs capping layer over electrons. The same mechanism also results in the 100 times stronger PL intensity of sample C than sample A. Similar results have also been observed in another literature of coupled GaSb QRs [13].

To further investigate the transition mechanisms of the samples, the 10 K PL spectra of samples A, B and C at a laser pumping power of 0.5 W/cm^2 are shown in Fig. 2(a). In this figure, except for the already observed red-shift peak with increasing In

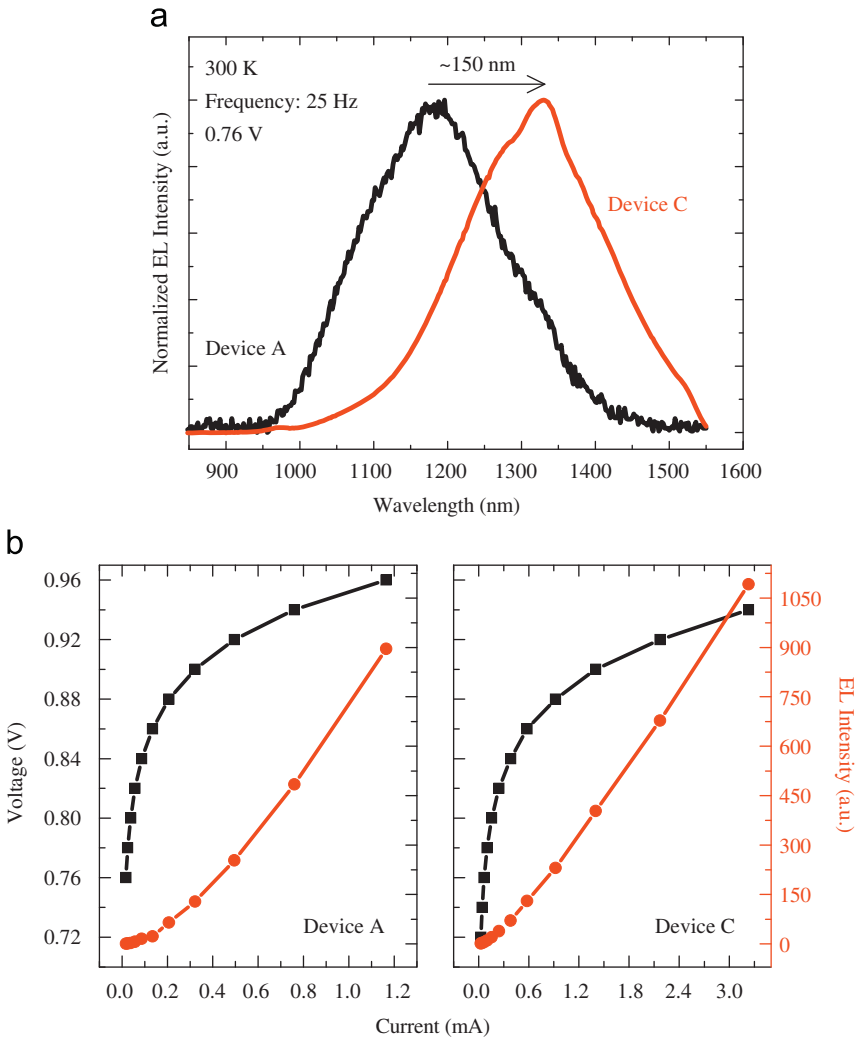

Fig. 4. (a) The room-temperature EL spectra at a 25-Hz pulsed voltage of 0.75 V and (b) The current–voltage (black filled squares) and light intensity–current (red filled circles) characteristics of devices A and C. (For interpretation of the references to color in this figure legend, the reader is referred to the web version of this article.)

composition, two distinct emission peaks in the shorter and longer wavelength sides are observed for each sample. To verify the transition mechanisms of the two peaks, power-dependent PL measurements were performed on the three samples at 10 K. The results are summarized and shown in Fig. 2(b). The two PL peaks of the three samples show linear dependence over the cubic root of laser pumping power density, which suggest that they are of type-II transitions [14,15]. In our growth method, the formation of GaSb QRs is due to Sb and background As exchange sequentially on the submit of GaSb QD during the post soaking procedure of Sb [12]. In this process, higher GaSb QDs are be transformed into QRs while smaller QDs may be transformed into wetting layers (WL) instead of QRs. In this case, the PL peak with a lower energy should be resulted from the QRs with the higher energy one from the WL. The other phenomenon observed in this figure is the similar energy difference of ~120 meV between the two PL peaks of the three samples. The result suggests the same influence of the conduction band-edge lowering of the InGaAs capping layers over the two PL peaks of samples B and C. The PL peak blue shifts of sample A, B and C in the same pumping power density span at 10 K for the QR and WL signals are 11/14, 26/22 and 27/28 meV, respectively. In the theoretical predication, the larger blue shift is resulted from higher carrier concentration accumulated in the type-II hetero-structure [14]. Due to the better confinement of the InGaAs layer in the conduction band, more electrons accumulated in the InGaAs layer are obtained. Therefore, the larger PL peak blue shift in the InGaAs-capped QR structures than that of the standard QR structure may be observed.

To clarify the transition mechanisms of the three samples, the schematic of band diagram of standard and InGaAs-capped GaSb QRs are shown in Fig. 3. As shown in Fig. 3(a), for standard GaSb QRs as the case of sample A, the electrons are loosely confined in the triangular well built in by the holes stored in GaSb QRs. The electrons may easily escape to bulk GaAs region. However, for InGaAs-capped QRs as the cases for samples B and C, the InGaAs capping layer provides a potential well for electron confinement. It will be more difficult for electrons to diffuse away from the (InGa)As/GaSb interfaces. This is the main reason why more intense PL intensities are observed for samples B and C. As for the transition mechanisms, since QR and WL signals are both observed in the 10 K PL spectra of the three samples, there should be at least three confinement states existed for sample A. They are $E_{\mathrm{hole,QR}}$, $E_{\mathrm{hole,WL}}$ and the confinement state $E_{\mathrm{electron,GaAs}}$ in the GaAs triangular well. The possible transition pathways for sample A should be between the $E_{\mathrm{electron,GaAs}}$ and $E_{\mathrm{hole,QR}}$/$E_{\mathrm{hole,WL}}$ as shown in Fig. 3(a). Compared with the 10 PL spectrum of sample A, the WL PL peak is missing from the 300 K PL spectrum. The phenomenon is attributed to the lower activation energy of the WL hole state such that the holes may diffuse out of the WL region easily at room temperature. As for the

case of InGaAs-capped QRs, the insertion of the lower-bandgap capping layers would provide a lower conduction-band edge such that the longer emission wavelengths are observed for samples B abd C. The InGaAs potential well will also provide a better electron confinement. Therefore, there should be at least four states existed for the InGaAs-capped QRs. They are $E_{hole,QR}$, $E_{hole,WL}$ and the confinement states $E_{electron,InGaAs}$ and $E_{hole,InGaAs}$ in the (InGa)As QW as shown in Fig. 3(b). The dominant transition pathways for InGaAs-capped QRs would become $E_{electron,InGaAs}-E_{hole,QR}$ and $E_{electron,InGaAs}-E_{hole,WL}$.

To demonstrate the possible applications of the type-II QR structures for the light-emitting diodes (LED), two GaAs PIN diodes with 3-period standard and $In_{0.15}Ga_{0.85}As$-capped GaSb QRs were prepared. The growth condition of the QR structures is the same as samples A and C. They are referred as devices A and C. After standard processing procedures, $630\times450\ \mu m^2$ mesas with a grid top contact metal were fabricated. The EL spectra of devices A and C operated at room temperature with a 25-Hz pulsed voltage of 0.75 V are shown in Fig. 4(a). Compared with device A, the EL peak wavelength of device C reveals a larger red shift of 150 nm, which is consistent with the large red shift of PL observation for sample C. The current versus voltage and light intensity versus current characteristics of devices A and C are shown in Fig. 4(b). According to this figure, it presents that device C gains a higher injection current and a more intense EL intensity at the same applied bias compared with device A. This result indicates that inserting an additional InGaAs QW layer into GaSb structure will not only extend the emission wavelength but also enhance the EL intensity. This is attributed to the fact that the electrons pass across to the active region, more electrons are attracted by the InGaAs QW instead of penetrating it due to its better quantum confinement. In this case, it increases the recombination probability of electron–hole pairs such that more intense EL intensity is observed for device C than that for device A. This result has demonstrated that the InGaAs-capped GaSb QRs is capable of the light-emitting device applications.

4. Conclusions

In conclusion, over 1.3 μm intense EL spectrum at room temperature of InGaAs-capped GaSb QRs is observed. By measuring the PL spectrum at low temperatures, the PL transition mechanisms for standard and InGaAs-capped GaSb QRs are further investigated. Compared with the standard GaSb QRs, InGaAs-capped GaSb QR structures exhibit a higher injection current and a more intense EL intensity. This result demonstrates the great potential of the structure in the application of near-infrared light-emitting devices.

Acknowledgment

This work is supported in part by the National Science Council, Taiwan under Grant number NSC 101-2628-E-001-001 and Nano-project granted by Academia Sinica.

References

[1] G.A. Sai-Halasz, L.L. Chang, J.M. Welter, C.A. Chang, L. Esaki, Solid State Communications 27 (1978) 935.
[2] H. Kroemer, G. Griffiths, IEEE Electron Device Letters 4 (1983) 20.
[3] F. Hatami, N.N. Ledentsov, M. Grundmann, J. Böhrer, F. Heinrichsdorff, M. Beer, D. Bimberg, S.S. Ruvimov, P. Werner, U. Gösele, J. Heydenreich, U. Richter, S.V. Ivanov, B.Ya. Meltser, P.S. Kop'ev, Zh.I. Alferov, Applied Physics Letters 67 (1995) 656.
[4] M. Geller, C. Kapteyn, L. Müller-Kirsch, R. Heitz, D. Bimberg, Applied Physics Letters 82 (2003) 2706.
[5] C.K. Sun, G. Wang, J.E. Bowers, B. Brar, H.R. Blank, H. Kroemer, M.H. Pilkuhn, Applied Physics Letters 68 (1996) 1543.
[6] J. Tatebayashi, A. Khoshakhlagh, S.H. Huang, G. Balakrishnan, L.R. Dawson, D.L. Huffaker, D.A. Bussian, H. Htoon, V. Klimov, Applied Physics Letters 90 (2007) 261115.
[7] K. Gradkowski, T.J. Ochalski, D.P. Williams, E.P. O'Reilly, G. Huyet, J. Tatebayashi, A. Khoshakhlagh, G. Balakrishnan, L.R. Dawson, D.L. Huffaker, Proceedings from SPIE Photonics West 6902 (2008) 17.
[8] E.P. Smakman, J.K. Garleff, R.J. Young, M. Hayne, P. Rambabu, P.M. Koenraad, Applied Physics Letters 100 (2012) 142116.
[9] R. Timm, H. Eisele, A. Lenz, L. Ivanova, G. Balakrishnan, D.L. Huffaker, M. Dähne, Physical Review Letters 101 (2008) 256101.
[10] P.J. Carringtona, A.S. Mahajumia, M.C. Wagenerb, J.R. Bothab, Q. Zhuanga, A. Kriera, Physica B: Condensed Matter 407 (2012) 1493.
[11] S.Y. Lin, C.C. Tseng, W.H. Lin, S.C. Mai, S.Y. Wu, S.H. Chen, J.I. Chyi, Applied Physics Letters 96 (2010) 123503.
[12] W.H. Lin, M.Y. Lin, S.Y. Wu, S.Y. Lin, IEEE Photonics Technology Letters 24 (2012) 1203.
[13] W.H. Lin, K.W. Wang, S.W. Chang, M.H. Shih, S.Y. Lin, Applied Physics Letters 101 (2012) 031906.
[14] D. Alonso-Álvarez, B. Alén, J.M. García, J.M. Ripalda, Applied Physics Letters 91 (2007) 263103.
[15] J. Tatebayashi, B.L. Liang, R.B. Laghumavarapu, D.A. Bussian, H. Htoon, V Klimov, G. Balakrishnan, L.R. Dawson, D.L. Huffaker, Nanotechnology 19 (2008) 295704.